



ENVIRONMENTAL RESEARCH BRIEF

Facilitated Transport of Inorganic Contaminants in Ground Water: Part II. Colloidal Transport

Robert W. Puls^a, Robert M. Powell^b, Don A. Clark^a and Cynthia J. Paul^b

ABSTRACT

This project consisted of both field and laboratory components. Field studies evaluated routine sampling procedures for determination of aqueous inorganic geochemistry and assessment of contaminant transport by colloidal mobility. Research at three different metal-contaminated sites has shown that 0.45 μm filtration has not removed potentially mobile colloids, when samples have been collected using low pumping flow rates ($\sim 0.2\text{-}0.3$ L/min). However, when pumping velocities greatly exceeded formation ground-water flow velocities, large differences between filtered and unfiltered samples were observed, and neither were representative of values obtained with the low flow-rate pumped samples. There was a strong inverse correlation between turbidity and representativeness of samples. Several different sampling devices were evaluated in wells (PVC) ranging in depths from 10 to 160 ft. Those devices which caused the least disturbance (i.e., turbidity) also produced the most reproducible samples irrespective of filtration. The following water quality indicators were monitored during well purging: dissolved O_2 , pH, Eh, temperature, specific conductance, and turbidity. Sampling was not initiated until all indicators had reached steady-state (usually ~ 2 to 3 casing volumes). In all cases turbidity was slowest to reach steady-state values, followed by dissolved oxygen and redox potential. Temperature, specific conductance, and pH results were generally insensitive to well purging variations.

^a U.S. EPA, Robert S. Kerr Environmental Research Laboratory, Ada, OK.

^b ManTech Environmental Technology, Inc., Robert S. Kerr Environmental Research Laboratory, Ada, OK.

In controlled laboratory experiments, the stability and transport of radio-labeled Fe_2O_3 model colloids were studied using batch and column techniques. Variables in the study included flow rate, pH, ionic strength, electrolyte composition (anion/cation), colloid concentration, and colloid size. Transport was highly dependent upon colloidal stability. Iron oxide colloids in the 100-900 nm particle diameter range were not only mobile to a significant extent, but under some hydrogeochemical conditions were transported faster than a conservative tracer, tritium. Extent of colloidal breakthrough was dependent upon a complex variety of parameters, however the highest statistical correlation was observed with particle size and anionic composition of the supporting electrolyte. The dissolved transport of arsenate, a ubiquitous priority metal contaminant at hazardous waste sites, was compared with that of colloid-associated arsenate transport. The rate of colloid-arsenate transport was over 21 times that of the dissolved arsenate.

INTRODUCTION

Understanding the transport and fate of inorganic contaminants in the subsurface environment has been complicated by recent field studies that show contaminant mobility to be greater than had been predicted. These predictions have been based on properties such as speciation, solubility, ion exchange, and sorption-desorption but have failed to account for the potential interactions between inorganic contaminants and mobile colloids. Colloids are generally considered to be particles with diameters less than 10 micrometers (Stumm and Morgan, 1981), and can include both organic and inorganic materials. In addition to having a high surface area per unit mass and volume, particles

of dissolved organic carbon, clay minerals and iron oxides are also extremely reactive sorbents for radionuclides and other contaminants. Drastic changes in aqueous geochemistry can bring about supersaturated conditions in which inorganic colloidal species are formed. Decreases in pH or changes in redox potential can cause the dissolution of soil or geologic matrix cementing agents, promoting the release of particles. Decreases in the ionic strength of the aqueous phase can enhance colloidal stability and promote their transport. If mobile, these particles may increase the mobility of sorbed contaminants above that predicted by our current simple dissolved-phase transport models.

Several studies have demonstrated the presence of such colloidal material in ground water, with indications that colloidal mobility may facilitate the transport of contaminants in some systems. These studies have also provided data on the size range of mobile colloids, with evidence that particles with diameters greater than 1 μm may actually move faster than the average ground-water flow velocity in porous media due to effects such as size exclusion from smaller pore spaces. Other studies have demonstrated the strong binding and enormous sorption capacities of colloidal particles for inorganic and organic contaminants. The significance of colloidal mobility as a contaminant transport mechanism ultimately depends on the presence of sufficient quantities of reactive particles in ground water. With current techniques, our ability to differentiate between naturally suspended particles and those which are brought artificially into suspension during sample acquisition is questionable.

Inherent to this problem is the arbitrary designation of 0.45 μm as an operational cutoff point for distinguishing between particulate and dissolved species. If particles as large as 1-2 μm are mobile, present in significant quantities, and capable of transporting contaminants long distances, then sampling protocols must quantify this component of transport. Transport models must then incorporate this mechanism to provide better contaminant migration predictions.

Colloidal Reactivity, Mobility and Size

Numerous studies demonstrate the strong adsorptive capabilities of secondary clay minerals, hydrous iron, aluminum and manganese oxides and humic material (Sheppard et al. 1979; Takayanagi and Wong, 1984; Sandhu and Mills, 1987; Means and Wijayarathne, 1982). In studies at underground nuclear-test cavities at the Nevada Test Site, Buddemeier and Rego (1986) found that virtually all of the activity of Mn, Co, Sb, Cs, Ce and Eu was associated with colloidal particles in ground-water samples. Sandhu and Mills (1987) found over 90% of the chromium and arsenic present in a laboratory column study was associated with colloidal iron and manganese oxide. Nelson et al. (1985) determined that colloidal organic carbon was a major factor controlling the distribution of plutonium between the solid and dissolved phases.

The mobility of these reactive particles has already been demonstrated. Gschwend and Reynolds (1987) concluded that submicron ferrous phosphate particles were suspended and presumably mobile in a sand and gravel aquifer. These particles were formed from sewage-derived phosphate that combined with iron released from aquifer solids by reduction and dissolution of ferric iron. Size distribution analyses indicated a large population of 100 nm particles, and a lesser quantity in the range 600-800 nm. In complementary laboratory experiments with sand columns

and carboxylated polystyrene beads ranging in size from 0.10 to 0.91 μm as model colloids, Reynolds (1985) recovered 45% of the 0.91 μm size beads, and greater than 70% of 0.10 and 0.28 μm size beads. Field studies by Nightingale and Bianchi (1977) showed that, under certain conditions, submicrometer-sized particles within the surface weathered zone were mobilized for some distance both vertically and laterally and affect ground-water turbidity. In laboratory tests, Eichholz et al. (1982) found that cationic nuclides were competitively adsorbed on suspended clay particles capable of travelling at bulk water flow velocity in porous mineral columns. Particulate matter of micrometer dimensions was shown to be responsible for the transport of radioactive sodium and ruthenium in sand beds by Champlin and Eichholz (1968). As much as 200 $\mu\text{g/L}$ copper, lead, and cadmium were found to be associated with colloidal material in the size range 0.015-0.450 μm by Tillekeratne et al. (1986). Rapid transport of plutonium in core column studies by Champ et al. (1982) was attributed to colloidal transport, with 48% of the plutonium associated with particles in the size range 0.003-0.050 μm and 23% in the range 0.050-0.450 μm .

Harvey et al. (1989) showed that, in a shallow sand and gravel aquifer, 1.35 μm latex particles traveled faster than the 0.23 μm size particles. This phenomenon was due to size exclusion effects (reduced path length), similar to what Enfield and Bengtsson (1988) observed in laboratory columns with organic macromolecules. Penrose et al. (1990) found detectable amounts of plutonium and americium, 3390 m downgradient from a source, to be tightly or irreversibly associated with particles between 0.025 and 0.45 μm in size. Champlin and Eichholz (1976) demonstrated that previously "fixed" particles and associated contaminants may be remobilized by changes in the aqueous geochemistry of the system. Cerda (1987) demonstrated that the mobilization of kaolinite fines in laboratory columns was almost totally dependent upon the chemistry of the fluids present, with maximum mobility occurring under relatively high saline, weakly alkaline pH conditions. Repulsive colloidal forces promoting stability were in evidence up to 0.1 M NaCl (pH 9). Matijevic et al. (1980) studied the stability and transport of hematite spheres through packed-bed columns of stainless-steel beads as a function of pH and the concentration of a variety of simple and complex electrolytes. Surface charge alterations of the hematite and stainless-steel beads by the different electrolytes was the dominant factor in colloidal deposition and detachment.

Recent estimates of colloidal concentrations in ground water range as high as 63 mg/L (Buddemeier and Hunt, 1988), 60 mg/L (Ryan and Gschwend, 1990), and 20 mg/L (Puls and Eychaner, 1990). Given the demonstrated high binding capacity of many of these particles, concentrations of this magnitude could have a significant impact on contaminant transport.

Dissolved vs. Particulate

Historically, 0.45 μm pore size filters have been used to differentiate between dissolved and particulate phases in water samples. If the intent of the filtration is to determine truly dissolved constituent concentrations for geochemical modeling purposes, the inclusion of colloidal material less than 0.45 μm in the filtrate will result in incorrect dissolved values. This result is often observed with iron and aluminum, where "dissolved" values are obtained that are thermodynamically impossible at the sample pH. Conversely, if the purpose of sampling is to estimate "mobile" species in solution, including both dissolved and particle-associated

contaminants, significant underestimations of mobility may result, due to removal of colloidal matter by 0.45 μm filtration.

Kim et al. (1984), found the majority of the concentrations of rare earth elements to be associated with colloidal species that passed through a 0.45 μm filter. Wagemann and Brunskill (1975) found more than two-fold differences in total iron and aluminum values between 0.05 and 0.45 μm filters of the same type. Some aluminum compounds, observed to pass through a 0.45 μm filter, were retained on a 0.10 μm filter, by Hem and Roberson (1967). Kennedy et al. (1974) found errors of an order of magnitude or more in the determination of dissolved concentrations of aluminum, iron, manganese and titanium using 0.45 μm filtration as an operational definition for "dissolved." Sources of error were attributed to filter passage of fine-grained clay particles.

Sampling Objectives and Recommendations

A common and overriding ground-water sampling objective is the acquisition of representative and accurate elemental concentrations for the purpose of risk assessment at hazardous waste sites. In addition to dissolved species, this should include contaminants sorbed to suspended (mobile) inorganic and organic particles. Disturbance of the subsurface environment is inevitable in the process of installing monitoring wells and collecting samples. Artifacts or contamination of samples can occur from the following: poor well design or construction; inadequate or improper well development; corrosion, degradation, or leaching of well construction materials; improper well purging, sampling, sample processing, transportation and storage. Intuitively, it makes sense to minimize disturbance of the sampling zone to obtain representative and accurate data. Excessive turbidity is the most common manifestation of disturbance. Turbidity results from stirred up or suspended sediment or foreign particles. Natural turbidity may exist where conditions are favorable for the production of stable suspensions (e.g. low ionic strength waters, geochemical supersaturation, high clay content), whereas excessively rapid pumping or purging relative to local hydrogeological conditions is the most common cause of artificial turbidity. Oxidation of anoxic or suboxic aquifer zones may result from high pumping rates which impact much larger segments of the aquifer than the interval of interest, causing the precipitation of iron oxyhydroxide and/or mixing of chemically distinct zones.

If a secondary objective is accurate "dissolved" elemental concentrations, then samples should be filtered in the field with in-line devices and using filter pore sizes $\leq 0.1 \mu\text{m}$.

Sampling recommendations consistent with the above discussions and recommendations were summarized in a previous Environmental Research Brief (Puls et al. 1990). Briefly these recommendations included:

- ◆ Isolation of the sampling zone with packers to minimize purge volume,
- ◆ Low flow rate pumping to minimize aeration and turbidity,
- ◆ Monitoring of water quality parameters while purging to establish baseline or steady-state conditions to initiate sampling,
- ◆ Maximize pump tubing wall thickness and minimize length to exclude atmospheric gases,
- ◆ Filtration for estimate of dissolved species and the collection of unfiltered samples for estimates of contaminant mobility.

FIELD STUDIES

Sites

Between June 1988, and February 1991, three different field sites were used to evaluate the above sampling techniques and recommendations, emphasizing the impacts of different sample collection devices on sample turbidity and filtration effects on metals concentrations. The first site is at Pinal Creek, near Globe, Arizona, about 130 km east of Phoenix and 170 km north of Tucson. This site and sampling results were discussed in detail in Puls et al. (1990).

The second is a Superfund site near Saco, Maine, about 30 km south of Portland and 7 km inland from the coast. This site was used for chromium waste disposal by a leather tannery from 1959 to 1977. Chromium wastes were dumped into 53 small unlined pits and two larger lagoons (each about 0.25 hectares). The site geology consists of glacial sediments, underlain by a sloping fractured bedrock surface. Sediment thickness ranges from 0 to 17 m. Analysis of ground-water flow is complicated by both the fractured nature of the bedrock and an apparent ground-water divide in the overburden. Upward gradients have been determined at some locations associated with ground-water discharge to surface drainages. Depth to water table ranges from 1 to 2 m below ground surface.

The third site is near Elizabeth City, North Carolina, about 100 km south of Norfolk, Virginia, and 60 km inland from the Outer Banks of North Carolina. A chrome plating shop, in use for more than 30 years, has discharged acidic chromium wastes into the soils and aquifer immediately below the shop. The site geology consists of typical Atlantic coastal plain sediments characterized by complex and variable sequences of surficial sands, silts and clays. Ground-water flow is generally to the northeast; however, in the immediate vicinity of the plating shop, flow appears to be directly toward the Pasquotank River about 90 m north of the shop. Ground-water flow is somewhat complicated due to wind tides. Depth to ground water is about 2 m. An estimated hydraulic conductivity value of 15 m/d was based on aquifer test data.

Site Sampling

The sampling set-up used at the Saco and Elizabeth City sites is depicted in Figure 1. This was similar to the arrangement used in Globe, where a laser light scattering instrument was used for tracking particle concentrations instead of a turbidimeter; and a bladder or submersible pump was used instead of a peristaltic pump (Puls et al. 1990). For comparison, a bailer was used in addition to the peristaltic pump at Saco and at Elizabeth City. A multiparameter instrument with flow-through cell was employed in all cases to monitor pH, temperature, specific conductance, redox potential, and dissolved oxygen during both purging and sample collection operations. Sample collection was initiated when all parameters, including turbidity, reached steady-state. Figure 2, for well MW101 at Saco, is typical of the trends for parameter equilibration during purging. Specific conductance, pH and temperature, although recommended by many sampling guidelines, were the least sensitive parameters, attaining steady-state values rather rapidly. Corresponding contaminant concentrations in addition to turbidity, redox, and dissolved oxygen, are also plotted in Figure 3 for well 1 at Elizabeth City. Chromate concentrations were shown to follow trends similar to those for equilibration-sensitive parameters.

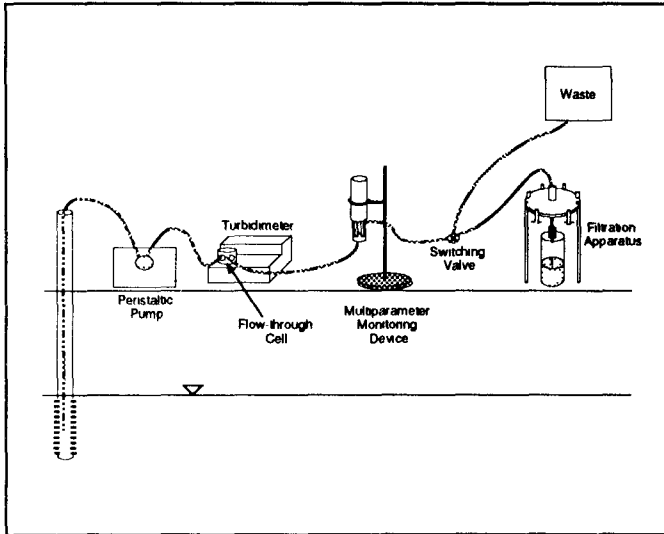


Figure 1. Sampling set-up for Saco, Maine, and Elizabeth City, North Carolina, sites (shallow wells).

Suspended Particles and Sampling Devices

At the Globe, Arizona site, comparisons were made between values of suspended particle concentration and particle size distributions using the following pumps: bladder (0.6-1.1 L/min), low speed submersible (2.8-3.8 L/min), and high speed submersible (12-92 L/min). Particle size distributions were measured with a laser light scattering instrument using photon correlation spectroscopy (Malvern AutoSizer IIC). Particles were captured on filters and identified by scanning electron microscopy with energy dispersive X-ray (SEM-EDX).

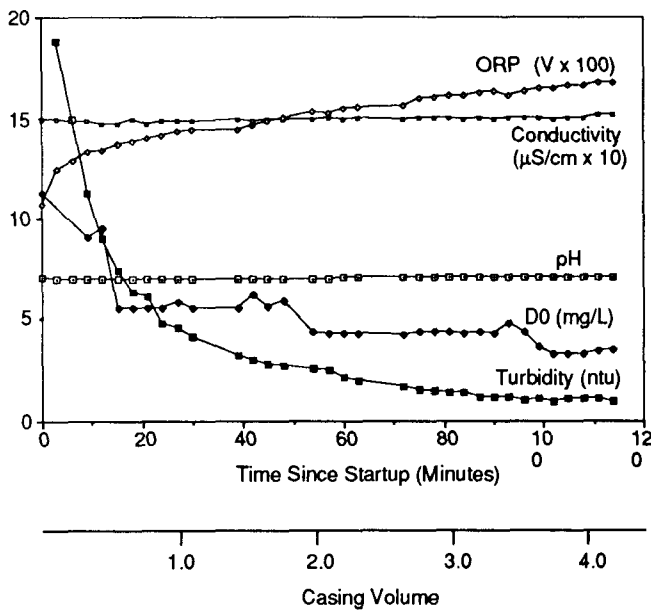


Figure 2. Equilibration of ground-water quality parameters during well purging (well MW 101, Saco, Maine, peristaltic pump (~0.2 L/min)).

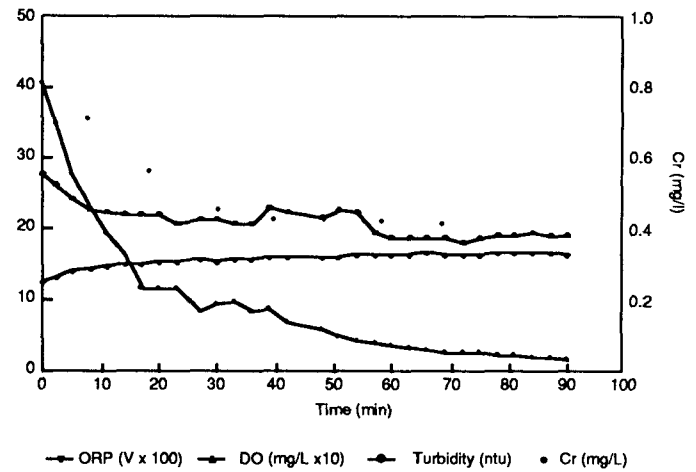


Figure 3. Equilibration of most sensitive ground water quality parameters and chromate concentration during well purging (well 1, Elizabeth City, North Carolina, peristaltic pump (~0.2 L/min)).

In well 105, more than 13 times more particles were mobilized by the low speed submersible pump compared to the bladder pump. This well is screened in the dense basin fill, where hydraulic conductivities are more than two orders of magnitude lower than those in the upper alluvium. Particles captured on filters were identified as iron-coated albite, gypsum and calcite. This lower region of the aquifer is saturated with respect to calcite, but unsaturated with gypsum. Gypsum particles were not present in the bladder pump samples, but were present in the submersible pump samples, probably due to mixing of the upper and lower aquifer waters caused by the relatively high pump rate. Differences in water chemistry from the bladder pump and high-speed submersible pump samples in June 1988, support this hypothesis (Brown, 1990). Interestingly, the calcite particles in the bladder pump samples were uniformly spherical and approximately 1 µm in diameter.

In well 452, screened in the alluvium, over 20 times more particles were mobilized by the high speed submersible pump compared to the bladder pump. These particles were captured on 0.1 µm filters and identified with SEM-EDX as predominantly smectite clays. Their presence was probably due to the fact that well 452 is screened in relatively fine grained sediment in the alluvium, and it is near the leading edge of the acidic waste plume where pH is decreasing rapidly and iron oxide coatings on colloidal clay are dissolving.

In well 503, also in the upper alluvium, successive use of the bladder, and the low speed and high speed submersible pumps produced increasingly more numerous and larger particles in suspension. The two low-discharge pumps produced monomodal particle size distributions of approximately 500 nm. The high discharge submersible pump produced larger particles in a bimodal distribution centered around 800 and 2000 nm because of increased turbulence. The predominant mineral identified on the filters from well 503 was gypsum. The upper alluvial aquifer is supersaturated with respect to gypsum due to the dissolution of calcite by sulfuric acid-dominated wastes which have leached into the subsurface for over 80 years.

Even with the bladder pump, particles brought to the surface were as large as 10 μm , probably too large to be naturally suspended in situ, but there was clearly a significant difference in particle population and size between the three different pumps. Increasing pump rate generally resulted in increased turbidity with larger particles brought into suspension. Some anomalous behavior in this regard was caused by the sequence of pump comparison in a given well (Puls et al. 1990).

A peristaltic pump was used at both the Saco, Maine and Elizabeth City, North Carolina sites because of the shallow depth to ground water. As a result, lower pumping rates were possible (0.2-0.3 L/min). Turbidity due to suspended colloids was measured with a turbidimeter equipped with flow-through cell (Figure 1). Turbidity is commonly measured in nephelometric turbidity units (NTUs) and based on the comparison of the intensity of light scattered by a sample with the intensity of light scattered by a standard reference suspension under the same conditions. Formazin polymer is used as the reference. Formazin has been found to be more reproducible than clay or natural water (Standard Methods for the Examination of Water and Wastewater, 1989). Jackson candle units (JCUs) were previously used with candle turbidimeters, and kaolin was a standard reference material. Table 1 lists correlations between NTUs, JTUs, and counts/1000/sec, as measured by two turbidimeters and a laser light scattering instrument respectively, using kaolinite as a common reference. Counts/1000/sec are photon counts recorded from laser light scattering measurements.

At Saco, most wells equilibrated at less than 5 NTUs; however, two wells equilibrated at 10 and 58 NTUs. The latter was an older well, and age or improper installation may explain the high turbidity value. At Elizabeth City, only 1 of 12 wells equilibrated at more than 5 NTUs. All of these wells were installed and developed by R.S. Kerr Laboratory personnel using best available technology and guidance. The well which had the highest equilibrated NTU value was well 8, the only well located (screened) in a clayey zone at the site (Figure 4).

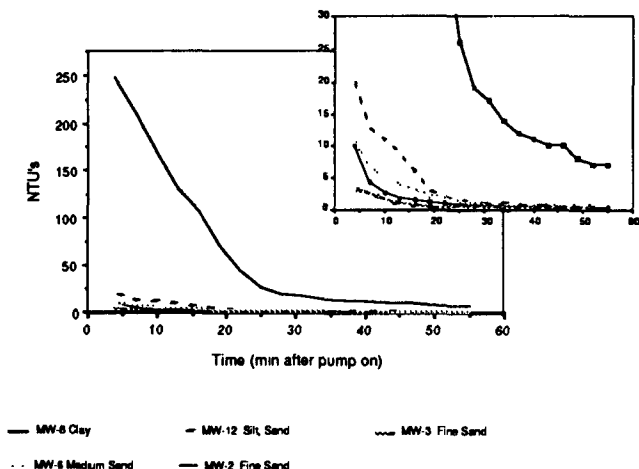


Figure 4. Equilibration of turbidity levels during well purging for several wells at the Elizabeth City site (peristaltic pump, ~0.2 L/min).

A down-hole camera was used at Elizabeth City during purging and sampling to evaluate the disturbance caused by emplacement and pumping. Little impact was observed when the peristaltic pump was turned on after both the pump tubing and the camera had been left in the screened interval overnight. Emplacement of the camera itself created the greatest turbidity and required overnight re-equilibration in the absence of pumping. Purging at low flow rate produced approximately the same result, in terms of turbidity, as did overnight equilibration. These observations argue strongly for dedicated sampling equipment as the optimal and perhaps most efficient manner of collecting representative ground-water samples.

Table 1. Comparison of nephelometric turbidity units (NTUs), Jackson candle units (JCUs), photon counts from laser light scattering (cts/1000/sec) and kaolinite concentrations in water (mg/L).

NTUs	JCUs	cts/1000/sec	mg/L
0.2	-	2.3	0.1
2.7	3.0	20.5	1.0
12.2	7.0	77.7	5.0
25.2	10.0	175.9	10.0
63.0	28.5	438.2	25.0
121.0	53.0	699.8	50.0
227.0	100.0	1412.2	100.0

Filtration and Sampling Devices

Filtration differences among the different sampling devices used at the Arizona site were generally not significant. Greater than 10% differences were observed in some wells, particularly with the high speed submersible pump, due to artifacts from the excessive turbidity created down-hole by the pump compared to the natural hydrogeological conditions (Puls et al. 1990). Similar filtration studies at Saco and Elizabeth City produced much more dramatic results.

Figure 5 shows chromium levels in samples from well 1 at Elizabeth City where samples were collected both with a peristaltic pump (200 ml/min) and with a bailer. The purge time for water quality parameter equilibration using the peristaltic was 1.3 hr, or about two casing volumes (Figure 3). Bailed samples were collected after a standard three casing volumes had been bailed. There were no significant differences in chromium concentrations between unfiltered and 5.0, 0.4 and 0.1 μm pore size filtered samples with the peristaltic pump. The bailed samples were not only significantly different, but were also 2 to 3 times higher than the peristaltic values. A similar response was observed in well 8. In all twelve wells, there were no differences observed in metal concentrations over the entire range from unfiltered to 0.1 μm -filtered, when the samples were collected with the peristaltic using a low pumping rate (~200 ml/min) and the set-up depicted in Figure 1.

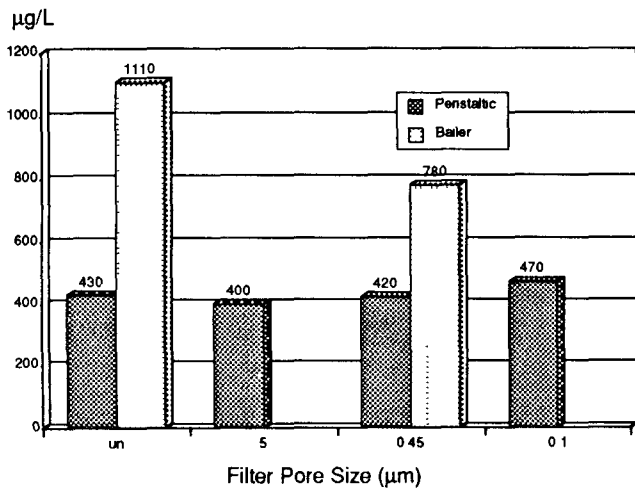


Figure 5. Differences in chromium concentrations for samples collected with peristaltic pump and bailer (well 1, Elizabeth City).

Although the Saco site is a chrome tannery waste disposal site, the inorganic contaminant of greatest interest in the ground water is arsenic. It is unclear at this time why the arsenic levels are elevated, and this is under further investigation. Figure 6 for well 113A shows arsenic levels for samples collected using both a peristaltic pump and a bailer. Results were similar to those for chromium at Elizabeth City. Once again, there were no differences observed in metal concentrations using the peristaltic pump and different filter pore sizes; but large differences were observed between filtered and unfiltered bailed samples. Also, these two sets of values were generally different from the peristaltic pump sampled values. The sampling set-up used with the peristaltic pump (Figure 1) consistently produced the most reproducible results, providing increased confidence that these samples were more representative of natural geochemical conditions and particle loading than those collected with the bailer.

It was interesting to note that there seems to be no significant contribution to contaminant transport from suspended and mobile particles greater than 0.1 µm at either the Elizabeth City or the Saco site. However, this does not indicate that colloidal facilitated transport by smaller particles may not occur at these sites.

LABORATORY STUDIES

Particles with diameters of 0.1 to 2.0 µm may constitute the most mobile size fraction in porous media. This is because the efficiency of particle removal increases rapidly above 1 µm diameter due to sedimentation and/or interception processes; whereas for particles smaller than 0.1 µm diameter, removal occurs primarily by diffusion (Yao et al. 1971 and O'Melia, 1980). Although significant contaminant transport by colloidal material in this size range was not observed for the above three sites, repeated particle size analyses using laser light scattering with photon correlation spectroscopy (PCS) for aqueous samples and scanning electron microscopy (SEM) analysis for particles collected on filters at the Globe site indicated a preponderance of particles in the size range 0.5 to 2.0 µm at the lowest flow rates used for sample collection. Because of these and similar observations by Gschwend and Reynolds (1987), laboratory experiments using alluvium from the Globe site were performed to investigate

specific aqueous chemical effects on the transport of environmentally realistic colloids, in the size range of 0.1-0.9 µm, through natural porous media under controlled conditions.

Iron oxide particles were synthesized to specific size and shape for use as the mobile colloidal phase in laboratory column experiments. The aquifer materials from Globe (wells 107 and 452) were used for the column packing or immobile phase. Arsenate was selected as a ubiquitous and hazardous inorganic contaminant, to study its interaction with both the porous immobile aquifer solids and the mobile inorganic colloids. Batch experiments were performed to evaluate colloid stability and assess the interactions between arsenate and colloidal Fe₂O₃, and arsenate and the aquifer matrix. Column experiments were performed to determine the extent of colloid transport and to compare retardation of aqueous and colloid-associated arsenate. Study variables included column flow rate, pH, ionic strength, electrolyte composition (anion/cation), colloid concentration and colloid size.

Characterization of Aquifer Solids and Colloidal Fe₂O₃

Core material from two locations at the site was used to pack 2.5-cm diameter, adjustable, glass columns. Prior to packing, the core sample was air-dried and sieved with the fraction between 106 and 2000 µm used in the columns. Subsamples were analyzed by X-ray diffraction. The predominant mineral phases, identified in order of intensity, were: quartz > albite >> magnesium orthoferrosilicate > muscovite > samsonite > manganese oxide.

The pH_{zpc}, or pH at which the net surface charge of a solid equals zero, is an important parameter affecting both colloidal stability and the interaction of the colloids with immobile matrix surfaces. Above the pH_{zpc}, minerals possess a net negative charge; while below this pH_{zpc}, the net charge is positive. Most sand and gravel-type aquifer solids exhibit a net negative charge under most environmentally-relevant pH conditions, due to the predominance of silica (pH_{zpc} ~ 2) and other minerals such as layer silicates and manganese oxides which have pH_{zpc}'s < 4.

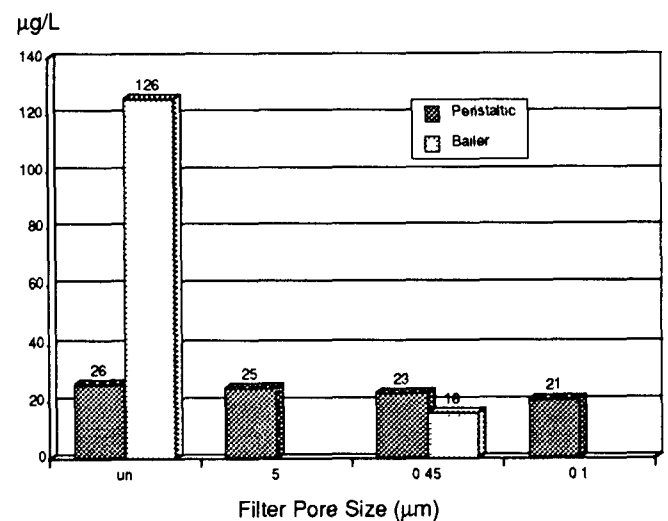


Figure 6. Differences in arsenic concentrations for samples collected with peristaltic pump and bailer (well 113A, Saco, Maine).

Spherical, monodisperse colloidal Fe_2O_3 (100-900 nm) was prepared from solutions of FeCl_3 and HCl using the method of Matijevic and Scheiner (1978). The method was modified by the addition of a spike of $^{59}\text{FeCl}_3$, prior to heating, to permit detection of the colloidal hematite with liquid scintillation counting techniques. The labeled colloidal Fe_2O_3 allowed unequivocal discrimination between injected particles and those mobilized within the column packing material.

Colloid concentration, in milligrams per liter (mg/L), was determined gravimetrically by both filtration and residue-on-evaporation techniques, coupled with solute analyses and mass-balance calculations. SEM and PCS were used to determine the particle size. PCS was also used to evaluate stability of the diluted colloidal suspensions and particle size in both influent and effluent column suspensions. The surface area of 200 nm diameter uniformly spherical hematite particles was calculated to be $5.72 \text{ m}^2/\text{g}$ using the equation,

$$A = \frac{6 \times 10^{-4}}{pd} \quad (1)$$

where A is the geometric surface area (m^2/g), p the density (g/cm^3), and d the diameter (cm).

The pH_{zpc} of the colloidal hematite was evaluated from acid-base titrations using varying concentrations of NaCl or NaClO_4 as the background (non-interacting) electrolytes. The plot in Figure 7a illustrates a distinct crossover in the titration curves at approximately pH 7.4 in NaCl . These titrations were performed in a nitrogen-filled glove box. Micro-electrophoretic mobility (EM) was used to evaluate the pH_{ipp} (isoelectric point) of the particles. This technique was performed in NaClO_4 . When only non-interacting electrolytes are present in solution, $\text{pH}_{\text{zpc}} = \text{pH}_{\text{ipp}}$. Therefore, this mobility measurement served to support the titration pH_{zpc} data (Figure 7b). The EM measurements were made on the bench in the presence of atmospheric CO_2 . Colloid stability in both influent and effluent column suspensions as well as in batch studies was also evaluated using PCS to monitor coagulation. The colloidal suspensions were stable in dilute NaClO_4 and NaCl over the pH ranges 2.0-6.5 and 7.6-11.0

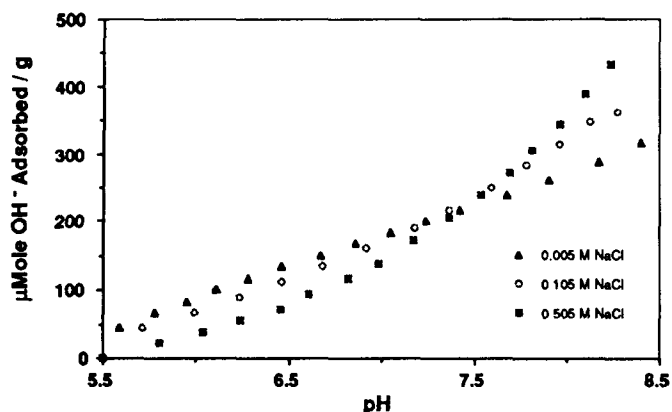


Figure 7a. Potentiometric titrations of Fe_2O_3 colloids as a function of pH in the presence of different concentrations of NaCl .

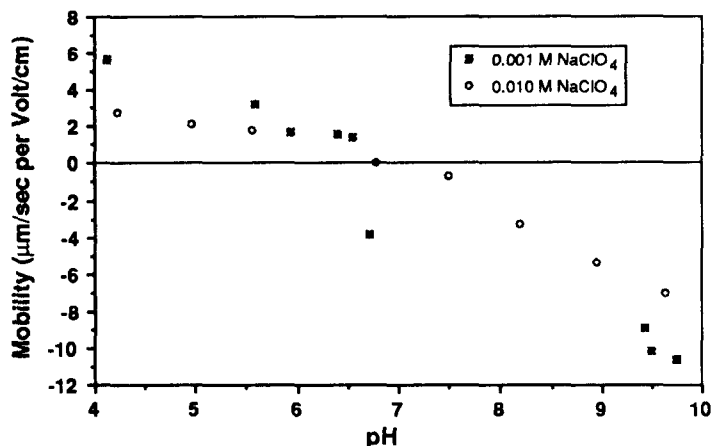


Figure 7b. Electrophoretic mobility of Fe_2O_3 colloids as a function of pH in the presence of different concentrations of NaClO_4 .

(Figure 8) respectively, with a region of instability corresponding to the estimated pH_{zpc} . Additional experimental details are provided in Puls et al. (1990).

In this study, significant enhancement of colloid stability in suspensions of $0.01 \text{ M Na}_2\text{HAsO}_4$, and $0.01 \text{ M NaH}_2\text{PO}_4$ was observed at pH values as low as 4 (\ll pristine pH_{zpc}) (Figure 9). This observation corresponds with work by Liang and Morgan (1990) who observed that hematite particles bear an overall net negative charge at $\text{pH} \ll \text{pH}_{\text{zpc,pristine}}$ in the presence of specifically sorbed anions (e.g. phosphate species). This phenomenon has the effect of increasing the stability region where the particles are negatively charged.

Arsenate Adsorption/Desorption

Adsorption of arsenate to the aquifer solids was performed to determine its affinity for these surfaces and to compare batch and column-derived solid-solution distribution values. Adsorption experiments with the colloidal hematite determined adsorption capacity and strength of arsenate retention. Adsorption data for arsenate on the aquifer solids were fitted to a Freundlich isotherm, defined by the relation

$$S = KC_i^n \quad (2)$$

where K is the empirical distribution coefficient or solid surface affinity term, S the steady-state concentration on the solids (mol/kg), C_i the steady-state solution concentration (mol/L), and n is an empirical coefficient related to the monolayer capacity and energy of adsorption. Steady-state, as used here, represents the pre-determined batch equilibration times (24 hr) where no continued decrease in aqueous arsenate concentrations within analytical uncertainty were observed. Values of $n < 1$ imply decreasing energy of sorption with increasing surface coverage. The calculated K and n values using the logarithmic form of the above equation were 5.5 and 0.73, respectively. These values represent relatively weak interaction with the aquifer solids, with the interaction primarily due to the presence of iron oxide coatings on mineral grains as determined by sequential extraction techniques (Tessier et al. 1979).

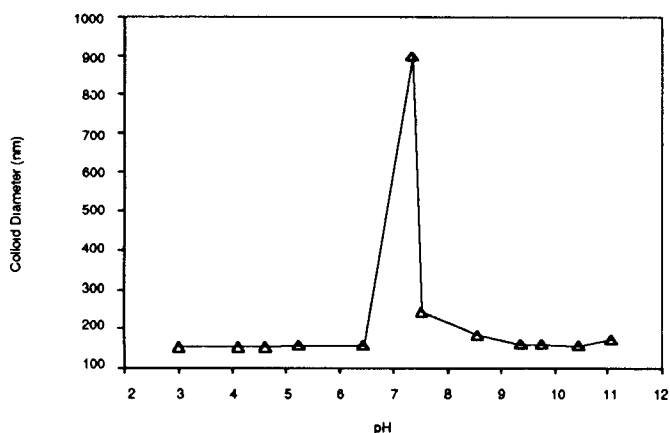


Figure 8. Stability of 150 nm Fe_2O_3 colloids as a function of pH in 0.005 M NaClO_4 .

Arsenate adsorption data for the Fe_2O_3 colloids were fitted to a Langmuir isotherm (Figure 10) defined by the relation

$$S = \frac{kbC_i}{1+kC_i} \quad (3)$$

where k is the Langmuir solid surface affinity coefficient, b the adsorption capacity, and S and C_i are defined above. An advantage of the Langmuir model is the incorporation of the capacity term. The correlation coefficient for the linearized Langmuir form of the above equation was 0.97 and the adsorption capacity was estimated to be 0.01 g arsenic/g Fe_2O_3 . There was very little difference in adsorption extent between pH 4-7. However, a gradual decrease was observed with increasing pH.

Desorption batch experiments were performed immediately following arsenate adsorption to simulate passage of an arsenate plume with subsequent contact by low-arsenate or arsenate-free water. An equivalent volume of arsenate-free 0.01 M NaClO_4

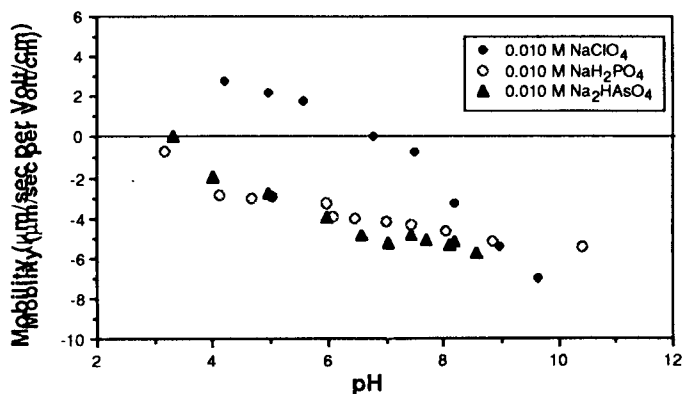


Figure 9. Electrophoretic mobility of Fe_2O_3 colloids as a function of pH in the presence of 0.01 M sodium electrolytes of different anionic composition.

was added to replace the extracted supernatant from adsorption batch reactors. The pH was the same pH used in the prior adsorption experiments (pH 7). Samples were equilibrated for 48 hrs. Strong retention of the arsenate on the hematite was observed, since only about 2-6% of the adsorbed arsenate fraction was released (Figure 11). Percent desorption was directly proportional to the initial arsenate concentration, indicating a decline in the energy of adsorption as the surface became increasingly saturated with arsenate. This phenomenon could have important implications for pump and treat remediation of highly contaminated sites. The easily desorbed arsenate will result in high initial efficiency of dissolved arsenate removal which may significantly decline once concentration values are reduced below the plateau portion of the adsorption isotherm and desorption becomes less energetically favorable.

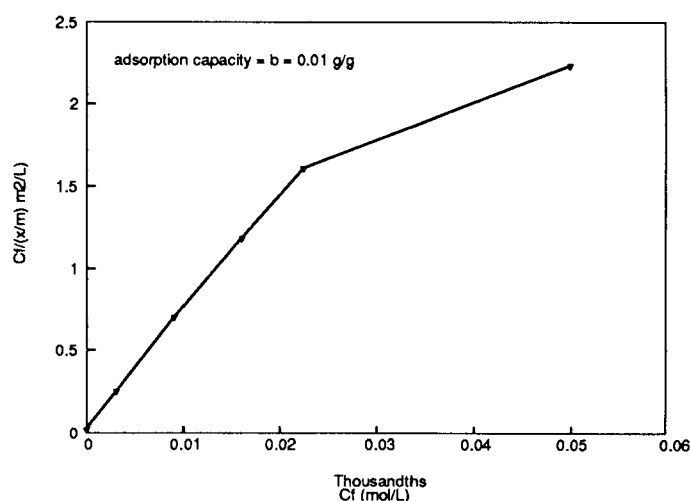


Figure 10. Langmuir isotherm data for arsenate adsorption on Fe_2O_3 colloids (pH 7, 0.01M NaClO_4 , 4.5 mg:30ml, 24 hr equilibration).

Dissolved Arsenate Transport

Column studies of dissolved arsenate transport were performed to compare distribution coefficients (K_d) with those derived from the batch tests and for comparison to Fe_2O_3 colloid-facilitated transport of the arsenate. Arsenate concentrations used in both sets of experiments were comparable. The column K_d roughly corresponds to the K value calculated from the batch tests and is determined by:

$$R_r = 1 + \frac{\rho_b K_d}{n} \quad (4)$$

where R_r is the retardation factor or ratio, v/v_c , of the velocity of the ground water to the velocity of the solute, ρ_b is the bulk density, and n is the porosity. Tritiated water was used for estimating the average water velocity.

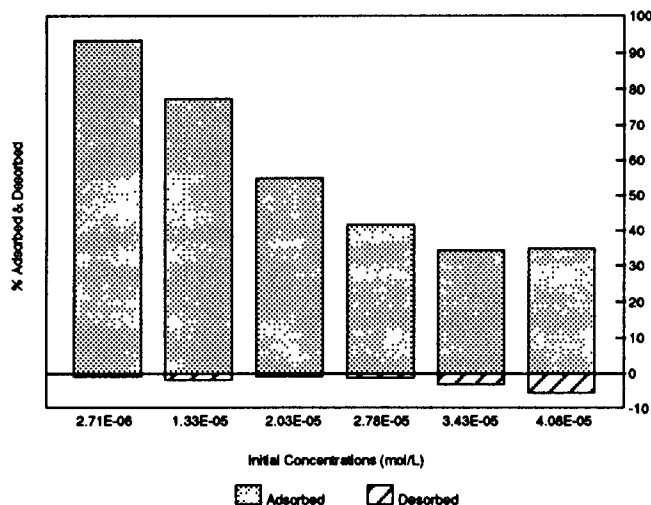


Figure 11. Adsorption-desorption data for arsenate on Fe_2O_3 colloids (pH 7, 0.01 M $NaClO_4$, 4.5 mg:30ml, 24 hr equilibrations).

As the flow velocity was decreased, the column K_d values approached those of the 24-hr equilibrated batch K values, indicating rate limited adsorption onto the aquifer solids at the higher flow velocities (Table 2). These results demonstrate the importance of generating comparative data and not relying solely on batch sorption static equilibrium data, especially for specific site assessment purposes. When ground-water flow velocities are relatively rapid, assumptions of local equilibrium may be invalid.

Following the arsenate transport experiments, the columns were flushed with deionized water (~zero ionic strength). This significantly increased turbidity in the column effluent due to dispersion of the colloidal aquifer fines. When the effluent was analyzed, the recovered arsenate was determined to be almost entirely colloid-associated and approximately equal to the influent arsenate concentration, demonstrating the potential importance of this transport mechanism (Figure 12).

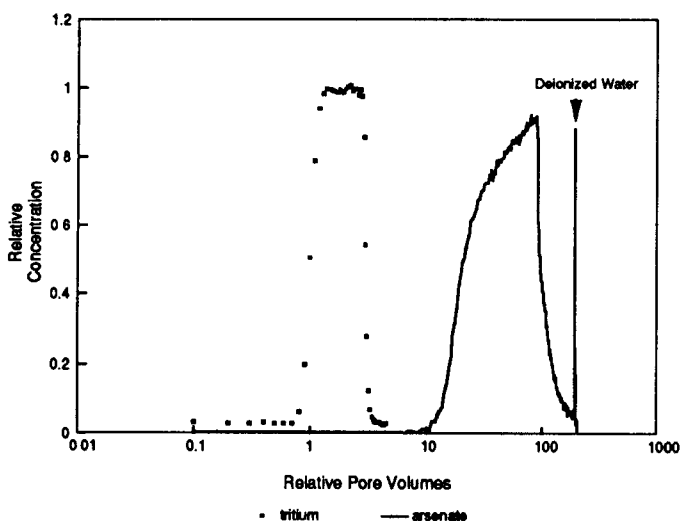


Figure 12. Breakthrough curve for dissolved arsenate versus tritium, and mobilization of colloidal-associated arsenate by deionized water.

Table 2. Comparison of distribution coefficients (K_d , L/kg) for arsenate using Globe, AZ aquifer material in batch and column tests ($p_b = 2.65 \text{ g/cm}^3$, $n = 0.4$).

Column		Batch
3.4 m/d	1.7 m/d	Steady-state
1.4	3.0	5.5

Colloidal Transport

Column flow rates used were comparable to estimated ground-water velocities in the Globe alluvium (0.8-3.4 m/d). The injected colloidal hematite generally broke through at the same time or prior to tritiated water (Figure 13). In this case, the rate of colloid transport through the columns was over 21 times faster than the dissolved arsenate. A summary of column results for the colloidal transport experiments has been compiled in Table 3. No colloid transport occurred when the particles were net positively-charged indicating significant electrostatic interaction with the net negatively-charged matrix material. In low ionic strength suspensions of $NaCl$ and $NaClO_4$, breakthrough exceeded 50% of initial colloid concentrations. These electrolyte suspensions were perhaps the most representative of natural conditions in uncontaminated ground water. There was substantially lower colloid recovery of sulfate-based suspensions, due to difficulties in maintaining colloid stability, and apparent non-specific interactions of the sulfate with the hematite surface.

Maximum percent breakthrough occurred with phosphate and arsenate-based suspensions and appeared to be unaffected by the range of flow velocities or column lengths used. Likewise, no significant differences were observed due to colloid concentration. The specific adsorption of the predominantly divalent phosphate and arsenate anions onto the hematite surface caused a charge reversal on the initially net positively-charged surface. The consequence is a lowering of the pH_{iep} below the pH_{zpc} value and an increase in net negative charge near the particle surface over a wider pH range. The increased negative charge increased repulsion between the mobile, negatively-charged particles, and the immobile, net negatively-charged, column matrix solids. As a result, the colloids were stable at a greater distance from the pore walls in the column matrix, where fluid velocity is higher.

Particle size had an inverse effect on percent breakthrough; that is, increasing colloidal transport was observed with decreasing particle size. While the larger particles were still transported there were significant differences between the 100 nm and 900 nm size classes. A complicating factor in resolving these differences was the use of a different aquifer solid sample (well 452) for the larger hematite particles. Sieve analyses of the two samples reflected differences in particle size (Figure 14), although XRD analyses showed no significant differences in mineralogy. The high density (5.3 g/cm^3) of the hematite may have contributed to gravitational settling of the larger particles. Densities of secondary clay minerals which are more representative of colloids in natural systems are on the order of 2.6 g/cm^3 .

Table 3. Column results of colloidal Fe₂O₃ transport through natural aquifer material

Size (nm)	pH	Velocity (m/d)	Part.Conc. (mg/L)	Ionic Strength	Anion	%C ₀ thru	Col. Length (cm)
200	3.9	3.4	10	0.005	Cl ⁻	0	3.8
125	8.9	3.4	10	0.005	Cl ⁻	54	5.1
150	8.1	3.4	5	0.001	ClO ₄ ⁻	57	3.8
250	8.1	3.4	10	0.03	SO ₄ ²⁻	17	3.8
150	8.9	3.4	5	0.03	SO ₄ ²⁻	14	3.8
100	7.6	3.4	5	0.03	HAsO ₄ ²⁻	97	2.5
100	7.6	1.7	5	0.03	HAsO ₄ ²⁻	96	2.5
100	7.6	0.8	5	0.03	HAsO ₄ ²⁻	93	2.5
125	7.6	3.4	10	0.03	HPO ₄ ²⁻	99	5.1
100	7.6	1.7	5	0.03	HPO ₄ ²⁻	99	2.5
100	7.6	3.4	5	0.03	HPO ₄ ²⁻	99	2.5
900	7.0	3.4	50	0.03	HPO ₄ ²⁻	33	3.8
900	7.0	3.4	50	0.03	HPO ₄ ²⁻	30	3.8

All of the parameters (Table 3 headings) or variables were explored in detail with the SAS program JMP, using %C₀ breakthrough as the response variable. Only colloid size and anion significantly impacted the %C₀ breakthrough. Combining these two parameters into a two-way main effects analysis of variance (2-way ANOVA) model accounted for 98.4% of the variability in the colloid breakthrough results. All other factors tested gave no significant correlation over the parameter ranges utilized in this study.

Given a ground water containing 10 mg/L suspended colloidal material, of surface area and reactivity comparable to these hematite particles, 0.1 mg/L of arsenic could be colloidal transported under some hydrogeochemical conditions. This is twice the maximum contaminant level (MCL) currently set for drinking water. It should be noted that these Fe₂O₃ model colloids are relatively non-reactive and have low surface area compared to the more ubiquitous subsurface colloidal minerals (e.g. clays, goethite). In addition, the suspended solids concentrations of these experiments were about one-half of those observed at the Arizona site and one-sixth the concentration observed at some other sites (Buddemeier and Hunt, 1988; Ryan and Gschwend, 1990).

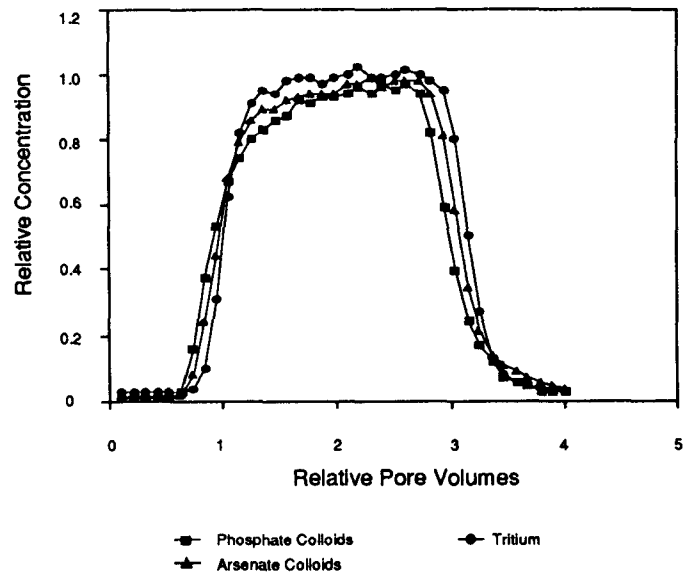


Figure 13. Breakthrough curve for Fe₂O₃ colloids suspended in 0.01 M NaH₂PO₄ and in 0.01 M Na₂HAsO₄, pH 7.6, 3.4 m/d, 5 mg/L.

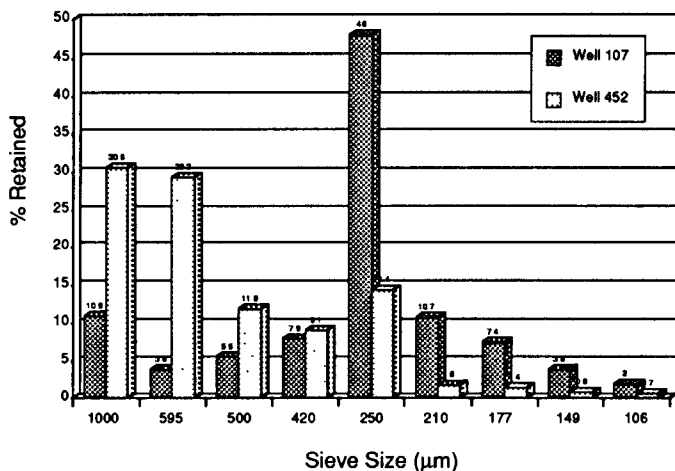


Figure 14. Sieve size fractionation of well 107 and well 452, Globe aquifer material.

SUMMARY AND CONCLUSIONS

Field results from three distinctly different sites indicate that the most representative and reproducible elemental concentrations are obtained by following the recommendations proposed previously by Puls et al. (1990). The selection of sampling devices, purging and sampling flow rates and filtration procedures are particularly important. There is a strong inverse correlation between turbidity and representativeness of samples. The greatest differences, both in terms of suspended colloids and inorganic contaminant concentrations, were observed between the bladder pump and the high speed submersible pump, in the deep wells, and between the peristaltic pump and the bailer in the shallow wells.

Steady-state turbidity levels observed at the three sites ranged from 1-58 NTUs; and in the case of one site, turbidity differences were strongly related to clay mineral content. Screened intervals with higher clay and silt contents had higher turbidity values. While artifacts of well construction and sample collection cause ground-water turbidity, there are indications that high levels of turbidity may occur naturally due to geology and geochemistry.

The down-hole camera indicated little artificial colloid generation or disturbance due to the low flow rate pumping action of the peristaltic pump. Emplacement of the camera, which is similar in size and shape to bladder pumps and submersible pumps, created the greatest disturbance (turbidity). While there has been no concrete evidence of significant colloidal-facilitated transport of inorganic contaminants at any of the three sites, the down-hole camera documented the existence of significant concentrations of suspended colloidal material in the flow field at Elizabeth City. Additional research in this area continues.

Laboratory experiments using natural aquifer material and realistic inorganic model colloids indicate that the transport of colloidal material through sand and gravel-type aquifers may be significant under certain hydrogeochemical conditions. Due to the strong reactivity of many inorganic colloids in natural subsurface systems, the potential exists that this form of contaminant transport may be important at certain sites. Its significance depends on a number

of chemical and physical variables, including but not limited to ionic strength, ionic composition, flow velocity, quantity, nature, and size of suspended colloids, geologic composition and structure, and ground-water chemistry. The most significant of these factors, under the conditions investigated in these column experiments, were ionic composition and particle size. Neglecting colloidal mobility in our predictive contaminant transport models may underestimate both the transport rate, maximum transport distance, and mass. Chemical parameters affecting colloidal stability and transport must be included in transport modeling along with physical parameters (such as pore size distribution, colloidal density and size, and flow velocity). Field sampling procedures must account for the possibility of colloidal transport and provide correct model input data. These concerns must be addressed during site characterization and assessment monitoring if colloid transport is deemed possible for the site.

REFERENCES

- Brown, J.G. Chemical, Geologic, and Hydrologic Data from the Study of Acidic Contamination in the Miami Wash-Pinal Creek Area, Arizona, USGS Open File Report, 90-395, October, 1990.
- Buddemeier, R.W. and J.H. Rego, Colloidal Radionuclides in Groundwater, FY85 Annual Report, Lawrence Livermore National Laboratory, Livermore, CA, UCAR 10062/85-1, 1986.
- Buddemeier, R.W. and J.R. Hunt, Transport of Colloidal Contaminants in Ground Water: Radionuclide Migration at the Nevada Test Site, Applied Geochemistry, 3:535-548, 1988.
- Cerda, C.M. Mobilization of Kaolinite Fines in Porous Media, Colloids and Surfaces, 27: 219-241, 1987.
- Champ, D.R., W.F. Merritt and J.L. Young, Potential for Rapid Transport of Pu in Groundwater as Demonstrated by Core Column Studies, In Scientific Basis for Radioactive Waste Management, Vol. 5, Elsevier Sci. Publ., NY, 1982.
- Champlin, J.B.F. and G.G. Eichholz, The Movement of Radioactive Sodium and Ruthenium through a Simulated Aquifer, Water Resour. Res., 4(1):147-158, 1968.
- Champlin, J.B.F. and G.G. Eichholz, Fixation and Remobilization of Trace Contaminants in Simulated Subsurface Aquifers, Health Physics, 30: 215-219, 1976.
- Eichholz, G.G., B.G. Wahlig, G.F. Powell and T.F. Craft, Subsurface Migration of Radioactive Waste Materials by Particulate Transport, Nuclear Tech., 58: 511-519, 1982.
- Enfield, C.G. and G. Bengtsson, Macromolecular Transport of Hydrophobic Contaminants in Aqueous Environments, Ground Water, 26(1): 64-70, 1988.
- Gschwend P.M. and M.D. Reynolds, Monodisperse Ferrous Phosphate Colloids in an Anoxic Groundwater Plume, J. of Contaminant Hydrol., 1:309-327, 1987.
- Harvey, R.W., L.H. George, R.L. Smith and D.R. LeBlanc, Transport of Microspheres and Indigenous Bacteria through a Sandy Aquifer: Results of Natural- and Forced-Gradient Tracer Experiments, Environ. Sci. Technol., 23(1):51-56, 1989.

Hem, J.D. and C.E. Roberson, Form and Stability of Aluminum Hydroxide Complexes in Dilute Solution, U.S. Geol. Water Supply Pap. 1827-A, A24, 1967.

Kennedy, V.C. and G.W. Zellweger, Filter Pore-Size Effects on the Analysis of Al, Fe, Mn, and Ti in Water, Water Resour. Res., 10(4): 785-790, 1974.

Kim, J.I., G. Buckau, F. Baumgartner, H.C. Moon and D. Lux, Colloid Generation and the Actinide Migration in Gorleben Groundwaters, In Scientific Basis for Nuclear Waste Management, V.7, Gary L. McVay, Ed., Elsevier, NY pp. 31-40, 1984.

Liang, L. and J.J. Morgan, Chemical Aspects of Iron Oxide Coagulation in Water: Laboratory Studies and Implications for Natural Systems, Aquatic Sciences, 52(1):32-55. 1990.

Matijevic, E. and P. Scheiner, Ferric Hydrrous Oxide Sols, J. Colloid Interface Sci., 63(3):509-524. 1978.

Matijevic, E., R.J. Kuo and H. Kolny, Stability and Deposition Phenomena of Monodispersed Hematite Sols, J. Colloid Interface Sci., 80(1):94-106. 1980.

Means, J.C. and R. Wijayarathne, Role of Natural Colloids in the Transport of Hydrophobic Pollutants, Science, 215(19):968-970, 1982.

Nelson, D.M., W.R. Penrose, J.O. Karttunen and P. Mehlhaff, Effects of Dissolved Organic Carbon on the Adsorption Properties of Plutonium in Natural Waters, Environ. Sci. Technol., 19: 127-131, 1985.

Nightingale, H.I. and W.C. Bianchi, Ground Water Turbidity Resulting from Artificial Recharge, Ground Water, 15(2): 146-152, 1977.

O'Melia, C.R., Aquasols: The Behavior of Small Particles in Aquatic Systems, Environ. Sci. Technol., 14(9):1052-1060, 1980.

Penrose, W.R., W.L. Polzer, E.H. Essington, D.M. Nelson and K.A. Orlandini, Mobility of Plutonium and Americium through a Shallow Aquifer in a Semiarid Region, Environ. Sci. Technol., 24:228-234, 1990.

Puls, R.W. and J.H. Eychaner, Sampling Ground Water for Inorganics - Pumping Rate, Filtration, and Oxidation Effects, In Fourth National Outdoor Action Conference on Aquifer Restoration, Ground Water Monitoring and Geophysical Methods, National Water Well Association, Dublin, OH, 1990.

Puls, R.W., J.H. Eychaner and R.M. Powell, Colloidal-Facilitated Transport of Inorganic Contaminants in Ground Water: Part I. Sampling Considerations, Environmental Research Brief, USEPA, EPA/600/M-90/023, December 1990.

Reynolds, M.D., Colloids in Groundwater, Masters Thesis, Mass. Inst. of Tech., Cambridge, MA, 1985.

Ryan, J.N. and P.M. Gschwend, Colloid Mobilization in Two Atlantic Coastal Plain Aquifers: Field Studies, Water Resour. Res., 1990.

Saltelli, A., A. Avogadro and G. Bidoglio, Americium Filtration in Glauconitic Sand Columns, Nuclear Technol., 67, 245-254, 1984.

Sandhu, S.S. and G.L. Mills, Kinetics and Mechanisms of the Release of Trace Inorganic Contaminants to Ground Water from Coal Ash Basins on the Savannah River Plant, Savannah River Ecology Lab. Aiken, SC, DOE/SR/15170--1, 1987.

Sheppard, J.C., M.J. Campbell and J.A. Kittrick, Retention of Neptunium, Americium and Curium by Diffusible Soil Particles, Environ. Sci. Technol., 13(6), 680-684 1979.

Standard Methods for the Examination of Water and Wastewater, 17th Edition, Clesceri, L.S., A.E. Greenberg and R.R. Trussell, Eds., American Public Health Assoc., Washington D.C., 1989.

Stumm, W. and J.J. Morgan, Aquatic Chemistry, John Wiley and Sons, Inc. N.Y., 1981.

Takayanagi, K. and G.T.F. Wong, Organic and Colloidal Selenium in South Chesapeake Bay and Adjacent Waters, Marine Chem., 14:141-148, 1984.

Tessier, A., P.G.C. Campbell, and M. Bisson, Sequential Extraction Procedure for the Speciation of Particulate Trace Metals, Anal. Chem., 51(7): 844-849, 1979.

Tillekeratne, S., T. Miwa and A. Mizuike, Determination of Traces of Heavy Metals in Positively Charged Inorganic Colloids in Fresh Water, Mikrochimica Acta, B:289-296, 1986.

Wagemann, R. and G.J. Brunskill, The Effect of Filter Pore-Size on Analytical Concentrations of Some Trace Elements in Filtrates of Natural Water, Intern. J. Environ. Anal. Chem., 4: 75-84, 1975.

Yao, K., M.T. Habibi and C.R. O'Melia, Water and Waste Water Filtration: Concepts and Applications, Environ. Sci. Technol., 5(11):1105-1112, 1971.

DISCLAIMER

The information in this document has been funded wholly or in part by the United States Environmental Protection Agency. This document has been subjected to the Agency's peer and administrative review and has been approved for publication as an EPA document.

QUALITY ASSURANCE STATEMENT

All research projects making conclusions or recommendations based on environmentally related measurements and funded by the Environmental Protection Agency are required to participate in the Agency Quality Assurance Program. This project was conducted under an approved Quality Assurance Program Plan. The procedures specified in this plan were used without exception. Information on the plan and documentation of the quality assurance activities and results are available from the Principal Investigator.

ACKNOWLEDGEMENTS

The authors wish to recognize and thank Dr. Terry F. Rees of USGS, San Diego, CA, for SEM-EDX analyses; Bert Bledsoe, RSKERL, for field assistance and much helpful technical assistance and guidance; Terry Connally and Dick Willey, USEPA, and Frank Blaha and Jim Vardy, USCG.